Health Monitoring of Composite Structures Using a Novel Fibre Optic Acoustic Emission Sensors

Badcock R.A., Krishnamurthy S., Fernando G.F., Butler T., Chen R., Tetlow J.

Engineering Systems Department, Cranfield University, Shrivenham, Swindon SN6 8LA UK

ABSTRACT

Acoustic emission (AE) is a well-established technique for non-destructive testing of engineering structures. It has been used widely to infer damage and failure processes in composite materials. In recent years, there has been significant activity globally in the development of fibre optic AE sensors for integrated health monitoring of composite structures, with many examples in the literature. Fibre optic based sensors have a number of advantages over conventional AE sensors, based on Lead Zirconium Titanate (PZT) piezo-electric transducers. For example, their circular cross-section makes it easy to embed them in composites, they offer immunity from electromagnetic interference and they can be multiplexed.

In this paper we report on the development and application of a new fibre optic AE sensor for health monitoring of composite structures. The sensor is based on a custom-made fused tapered coupler. The sensor is fabricated by thermally fusing two optical fibres and subsequently drawing them until the required coupling ratio between the fibres is reached. The sensor principle is based on the change in the coupling ratio of the fused tapered coupler when it interacts with an AE event. The variation in coupling ratio is detected by monitoring the light intensity at the output ports of the coupler in conjunction with appropriate signal processing.

The sensitivity and performance of the fibre optic sensor is compared to conventional PZT transducers. The procedures for surface mounting the sensors within or on composite materials are presented. In this paper we correlate the AE recorded by surface-mounted fibre optic AE sensors with the various damage events occurring in a glass fibre-reinforced composite material during mechanical testing. Damage in the composite was also studied by microscopic and edge-replication techniques.

1. INTRODUCTION

Acoustic emission-based condition monitoring of load-bearing structures, materials and machinery is a well established field with piezo-electric (lead-zirconium-titanate (PZT)) transducers dominating this technology. Their long-history has resulted in sophisticated and sensitive sensors along with robust instrumentation and a range of data analysis routines. The limitation of the conventional acoustic emission (AE) sensor systems for *in-situ* damage detection are: (i) limited operational temperature range; (ii) their large dimensions means that it is difficult or not acceptable for them to be embedded in fibre reinforced composites; (iii) the sensors are susceptible to electromagnetic interference and the protective measures needed to combat this means a significant increase in weight; and (iv) as they are surface-mounted devices, a coupling medium has to be used to secure the sensor to the material. The nature of the couplant, the thickness and void content at the interface can influence the AE data. Therefore, these surface-mounted devices are not necessarily suitable for long term *in*-situ structural integrity monitoring. With reference to optical fibre-based AE sensor systems, significant progress has been made over the last decade in their development. The most popular fibre optic sensor systems are based on two-beam interferometers: these are extremely sensitive to AE but unfortunately, they are also sensitive to vibration, temperature and strain. Furthermore, the instruments used for interrogating the sensors are not suitable for on-site applications. This current paper reports on a simple and highly cost-effective optical fibre-based AE sensor system, which does not have the disadvantages, mentioned above. The proposed sensor design is best described as consisting of two optical fibres that have been fused (joined at a specified region) and then drawn to form a tapered section. The term "fused tapered

coupler" will be used to describe this sensor design. A schematic illustration of the sensor is presented in **Figure 1**.

2. EXPERIMENTAL

2.1 Materials

The material used in this study was a 16-layer cross-ply glass fibre composite with the following lay-up sequence $[(0/90)_2(90/0)_2]S$. The prepreg (Hexcel 913G-E-5-30%) was laminated and processed in an autoclave using conventional procedures and the cure schedule recommended by the manufacturer. Post-processing, the composite panel was C-scanned, cut into rectangular strips of 250 mm by 20 mm and prepared for end-tabbing. Longitudinal edges of a selected number of samples were polished down to 0.25 μm to enable edge-replication via polyvinylacetate and acetone during the hold period of the ramp-hold sequence. All the test specimens were end-tabbed using 2 mm aluminium and stored in a dessicator until required.

2.2 Sensors

Electrical resistance strain gauges: All the specimens were instrumented with an electrical resistance strain gauge (ERSG) of type FLA-6-11 with a 2.12 gauge factor from TML Techni Measurement Limited, Warwickshire).

Fibre optic AE sensors: The fibre optic AE sensors were manufactured in-house using a custom-modified coupler manufacturing rig (Joinwit JW2000A). This rig is used commercially to manufacture couplers for optical fibre-based applications. However, in the current application, the fused tapered region is manufactured such that it is sensitive to acoustic waves. In summary[1], two lengths of Fibercore SM600 single mode fibre are stripped 20 mm around their centre point and clamped in the coupler fabrication rig. Prior to clamping, a twist is applied to the pair of optical fibres to bring them in to intimate contact. A hydrogen flame was then introduced and the fibres were drawn apart by a specified distance. The sensors for surface-mounted applications were packaged in a silica v-groove and secured in position using UV epoxy (UV403-T from Shanghai Jiyuan Ltd). The relative dimensions of the packaging medium was a 0.8 mm groove with outer dimensions of 1.5 by 1.0 mm. With regards to embedded sensor applications, a silica capillary tube was slid over the fused tapered region and secured in place using the above-mentioned UV resin.

2.3 Test methodology

Mechanical testing: The tensile tests were carried out on an Instron 1195 at a cross-head displacement rate of 2 mm/min at 23 °C. Two basic experiments were carried out; ramp-holds and quasi-static test to failure.

Sensor evaluation: The performance of the optical fibre AE sensors were evaluated using three basic test methods. The first involved the use of the ubiquitous pencil-break test where a 2H, (0.5 mm) pencil lead was fractured at a specified distance from the optical fibre sensor. The response from the surface-mounted PZT sensor was used for comparison purposes. These initial tests were carried out prior to, and subsequent to, loading the samples on the mechanical test machine. In the second set of tests, the sample was subjected to a series of mechanical load/holds; the hold period enabled edge replicas to be obtained. In the final set of tests, the samples with the optical and PZT sensors were loaded to failure. The relative positions of the optical and ERSG on the test specimen is shown in Figure 1. The location of the pencil-breaks on the tests specimen is indicated in Figure 1 with the codes A, B and C. The relative dimensions of the key components in the test specimen are also indicated in Figure 1.

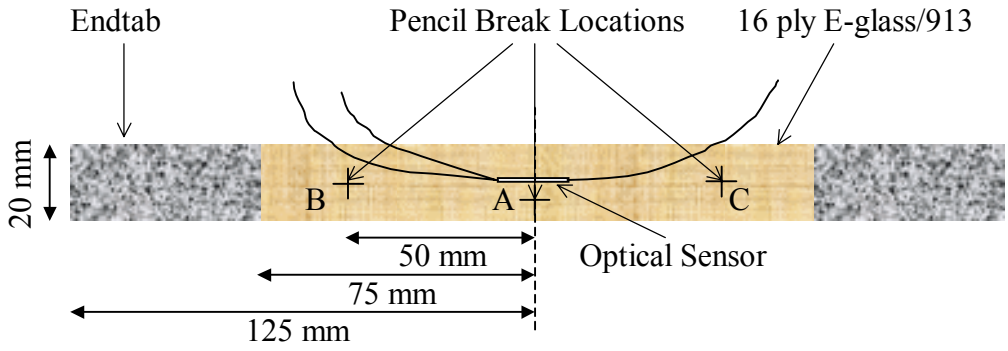

Figure 1 Positions of the sensors and locations of 'pencil break' simulated AE.

Damage detection: Edge replicas of the polished edges were taken using strips of polyvinyl acetate and acetone during the hold period of mechanical loading. A surface-mounted PZT sensor (Physical Acoustics R15) was used in conjunction with the optical fibre-based AE sensors. The PZT sensor was interrogated using a Physical Acoustics Mi-Tra and Mistras system with the following instrument and data acquisition parameters: sample rate of 10MHz, band-pass filter of 10kHz (low) and 1200kHz (high), delay of 100 μseconds and 10,000 data points. The optical fibre AE sensor was connected to the above-mentioned interrogation via a custom-designed optical/electrical interface that implements an optical ratiometric detection scheme. A schematic illustration of the experimental set-up is presented in Figure 2. With reference to Figure 2, a PZT transducer was mounted 10 mm from the centre of the test specimens and the specimen mounted in the grips of an Instron 1195 tensile test machine. A fibre-coupled 635 nm laser diode was spliced to the input fibre of the FOS and the FOS interrogated using a custom designed ratiometric detector. The PZT transducer was connected to a Physical Acoustics model 2/4/6 preamplifier and both optical and PZT AE signals connected to the AE interrogation system.

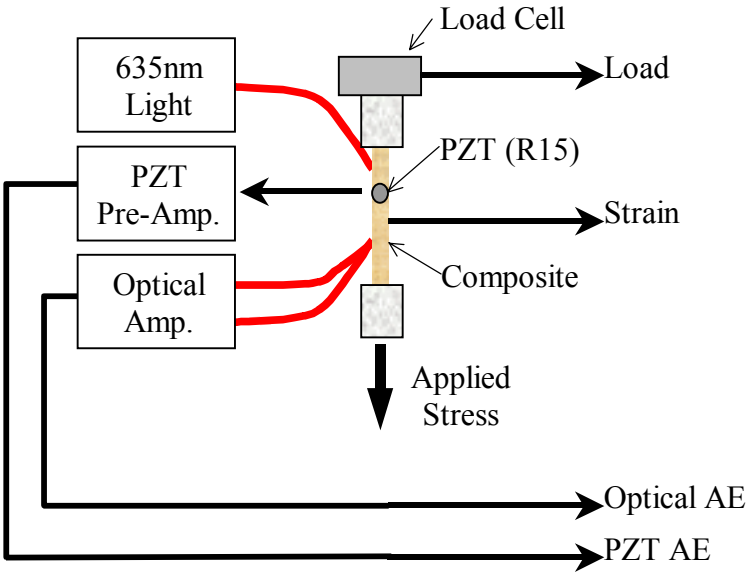

Figure 2 Schematic illustration of the experimental set-up.

3. RESULTS AND DISCUSSION

Figure 3 (a, b and c) represent typical responses of the fibre optic AE sensor (FOS) to a pencil-break test at positions A, B and C on the test specimen. These series of tests represent an average of six individual pencil-breaks and the data are summarised in Table 1.

Table 1 Sensitivity data for FOS tested.

Sensor	*Position*	*Noise (V)*	*Amplitude (V)*	*SNR (dB)*
6-02-2004-2 Silicone bond	A	4.78E-04	2.0	72.5
	B	4.76E-04	1.4	69.1
	C	5.34E-04	1.0	65.5
	PZT	9.44E-06	4.8	114.1
23-4-2004-5 Silicone Bond	A	2.24E-03	2.7	61.7
	B	2.04E-03	1.7	58.7
	C	2.06E-03	1.3	55.7
	PZT	2.17E-05	3.0	102.9
23-4-2004-4 Cyanoacrylate Bond	A	1.40E-03	2.1	63.7
	B	1.20E-03	0.7	54.9
	C	1.28E-03	0.5	52.2
	PZT	2.17E-05	3.0	102.9
01-04-2004-2 Epoxy Bond	A	2.21E-03	2.1	59.8
	B	1.28E-03	0.7	55
	C	1.13E-03	1.1	59.4
	PZT	2.96E-05	4.6	103.8
tb_20April1 Epoxy Bond	A	1.1E-03	3.5	70.1
	B	8.57E-04	1.3	63.9
	C	9.38E-04	1.7	65
	PZT	2.96E-05	4.6	103.8
tb_22April4 Epoxy Bond	A	8.19E-04	1.4	64.4
	B	8.57E-04	0.7	58.8
	C	8.94E-04	0.6	57
	PZT	1.29E-04	4.6	91
tb_22April5 Epoxy bond	A	1.68E-03	0.8	53.4
	B	1.59E-03	0.3	45.6
	C	1.74E-03	0.3	44.6
	PZT	1.73E-05	2.9	104.4

The response from a surface-mounted PZT sensor located 10 mm from the centre of the specimen is also presented to aid a comparison between the two sensor systems. The general form of the AE data detected by the FOS at positions A, B and C were characteristically different. However, the nature of the waveform at each position for the six individual pencil-breaks were similar. For example, position A registered the highest output intensity with the initial signal showing the largest amplitude. With reference to positions B and C, the signal was seen to rise for approximately 150 μseconds and it reached a maximum followed by a steady decay. Similar pencil-break tests were carried out using different materials as the bonding medium to secure the FOS on the surface of the composite, see summary in Table 1. It is readily apparent that the FOS exhibits "directional sensitivity". In other words, the AE signal detected by the FOS that was located at the centre of the test specimen, was found to be dependent on the position of the pencil-breaks (positions B and C (see Figure 1). This may be attributed to the increased distance between pencil break and sensor and to asymmetry in the packaged sensor system. The packaged sensor has a complex structure involving a number of (i) interfaces, (ii) material types and (iii) geometrical profiles along its length. Whilst every attempt was made to control the relevant parameters during the fabrication of the FOS, the data presented in Table 1 suggests the need for tighter control over the sensor fabrication and packaging operations. The relevant data for the response of the PZT to a pencil-break is also presented in Table 1. The relative sensitivity of the OFS is less than that obtained by the PZT. This can be partly explained by the increased noise level in the OFS compared to that of the PZT as summarised in Table 1.

On examination of the frequency spectrum for the data presented in Figure 3 (a-c) some differences could be observed. The frequency content at location A (see Figure 3a) was mostly below 200 kHz and those at B and C were below 100 kHz. Further studies are required to fully correlate the frequency response of the sensor for different positions on the test coupon.

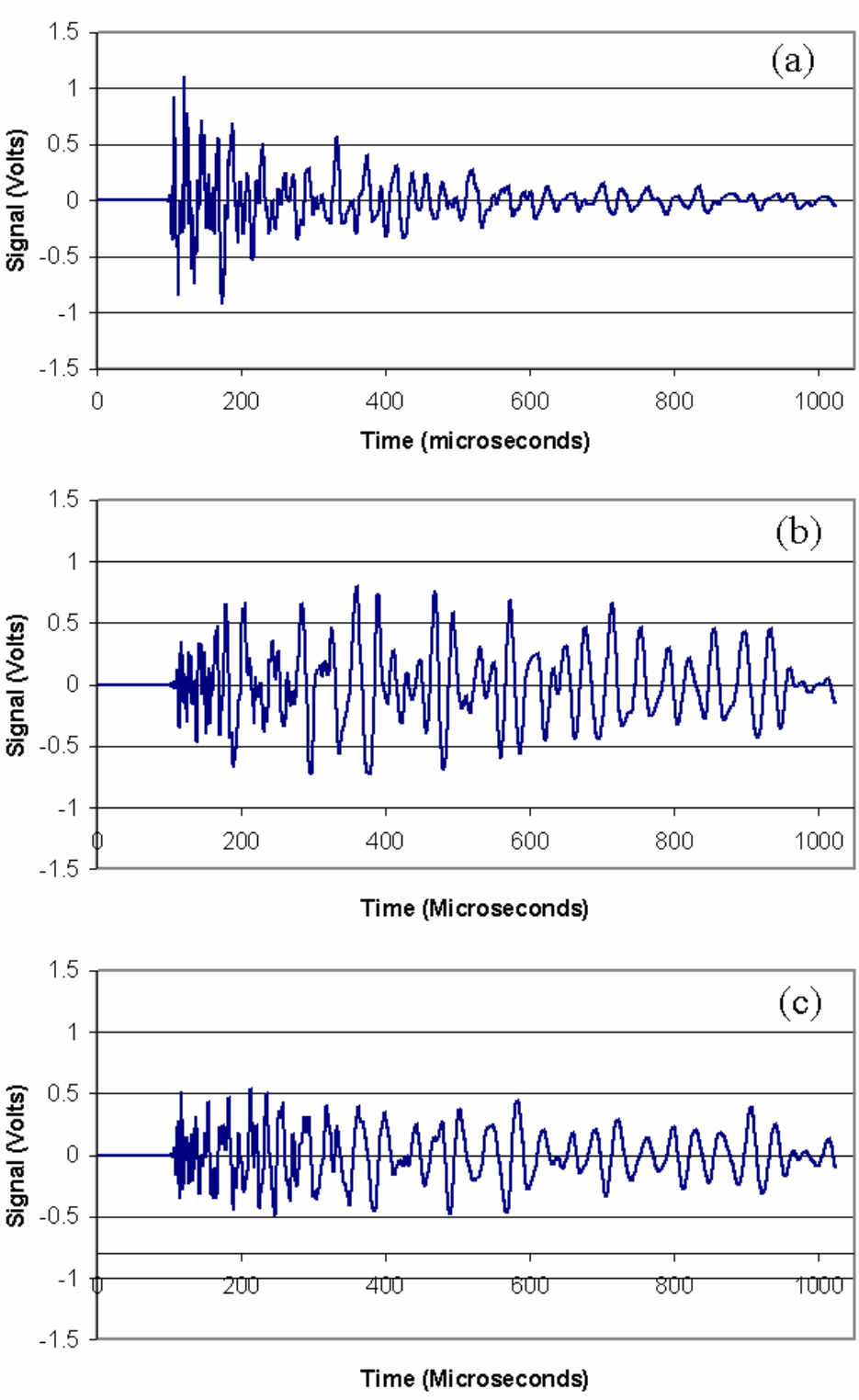

Figure 3 Response of the FOS to a pencil-break at positions A (a), B (b) and C (c).

Table 2 Comparison of FOS bonding conditions and signal transmission with distance.

Sensor ID	A / PZT	B / A	C / A	Bonding Condition
01-04-2004-2	0.53	0.34	0.49	2011 epoxy
tb_20April1	0.12	0.38	0.47	2011 epoxy
tb_22April4	0.15	0.55	0.47	2011 epoxy
tb_22April5	0.12	0.39	0.38	2011 epoxy
23-4-2004-5	0.67	0.64	0.46	silicone
6-02-2004-2	0.53	0.67	0.50	silicone
23-4-2004-4	0.57	0.31	0.25	cyanoacrylate

Table 2 presents a comparison of the AE data obtained using the PZT mounted with grease (Loctite Super Lube) and OFS that were each surface-mounted with different adhesives. The relative signal for an optical sensor when compared to PZT and the attenuation experienced by the OFS in moving the pencil-breaks from positions A to B and C, respectively, is summarised in Table 2. Further consideration is being given to the nature of the interaction of the packaged sensor in/on the composite and the predominant wave propagation modes and reflections in the composite and the sensor system.

The effect of the adhesive on the coupling efficiency of the acoustic energy between the packages sensor and the composite is apparent. At the time of writing, it was not possible to attribute specific reasons for the observed trend in the OFS. The difficulties in decoupling the relative contributions from the following factors is acknowledged and warrants a detailed study: (i) sensor to sensor variation as a consequence of the fabrication procedures used; (ii) variability in controlling the various parameters such as the tension on the sensor, the glue line thickness, the relative acoustic impedance match between the sensor and the packaging materials and the symmetry of the fused tapered coupler; (iii) selection of the material used to bond the sensor to the substrate.

Figure 4 illustrates a typical output from a conventional PZT during a quasi-static tensile test using a 16-layered cross-ply glass fibre/epoxy composite. In the subsequent tests, the term "hits", "energy" and amplitude are defined as follows: an AE hit describes the detection and measurement of an AE signal, AE amplitude is the largest voltage peak in the AE signal waveform, AE Energy is taken as the area under the signal curve. The strain data were obtained using ERSG and the failure strain of these devices was approximately 3%.

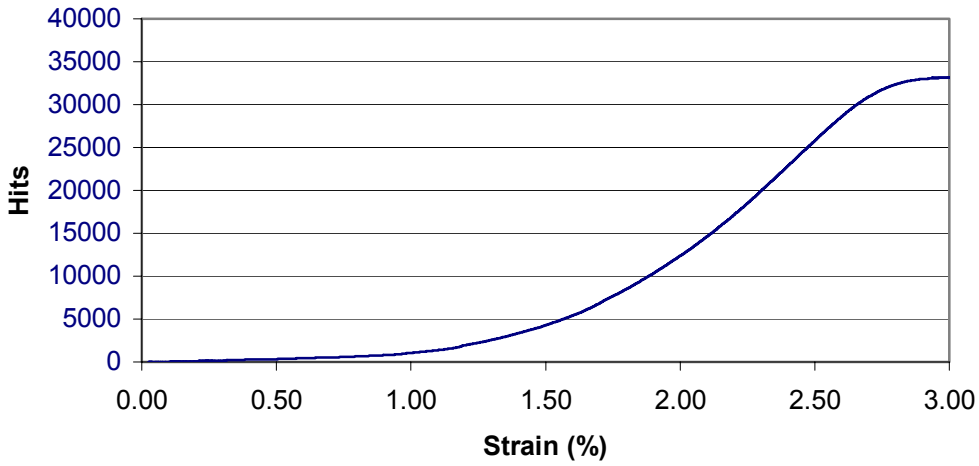

Figure 4 AE response of PZT during static tensile testing of a cross-ply E-glass composite.

Figure 5 shows the output from the PZT during a mechanical test where the applied load was held periodically to enable edge replicas to be obtained. The load-drop-off during the hold period and the generation of AE events during the ramp phase is evident.

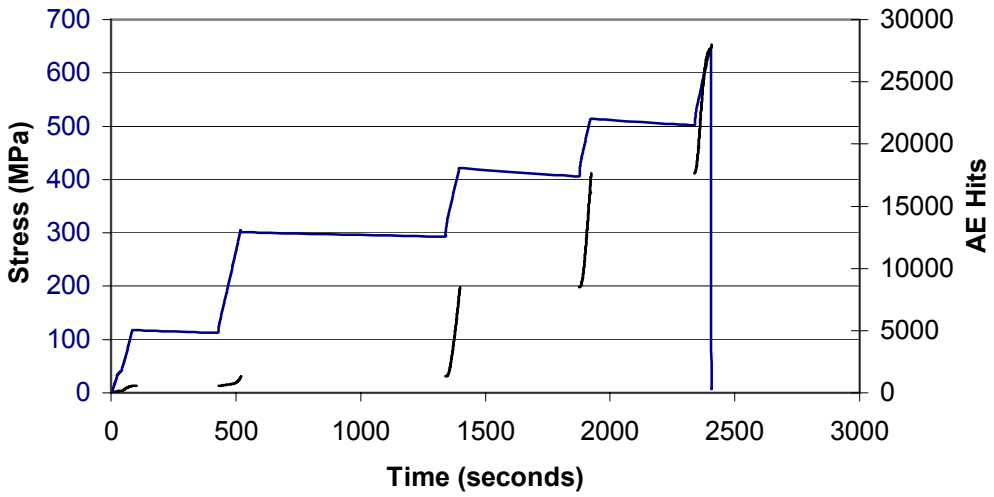

Figure 5 Relationship between stress, AE activity and time for a PZT sensor mounted on a cross-ply composite coupon 'ramp and hold' tested to failure.

The energy distribution and amplitude for this data set are presented in Figure 6. It is apparent from this data that for higher stress levels, increasing numbers of higher energy and amplitude hits are detected from the composite. One feature of these plots is the 'knee' in the energy and amplitude above a stress level of 420 MPa.

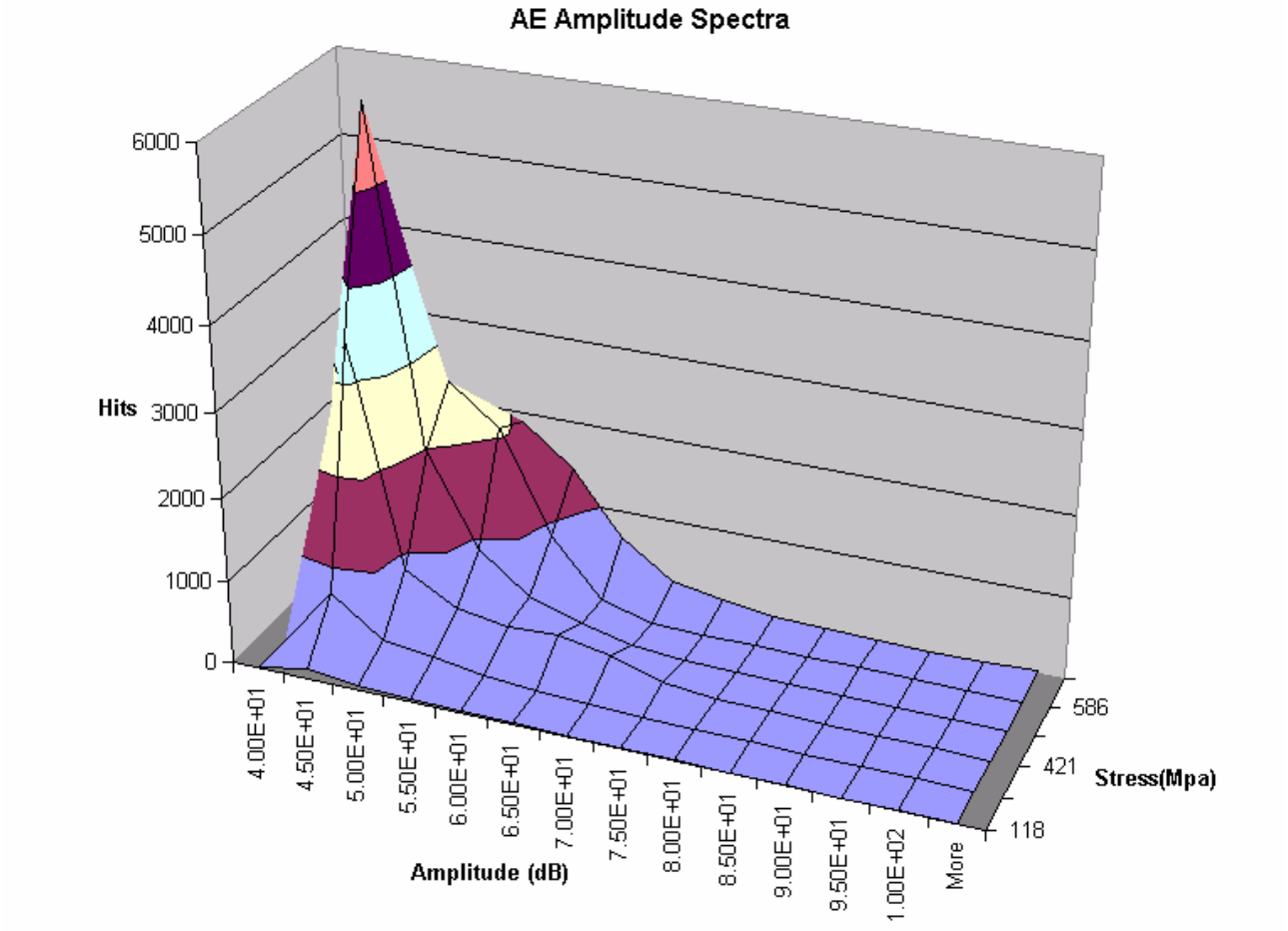

Figure 6 AE amplitude spectra with increasing stress.

Figure 7 illustrates the situation where the PZT was active during the load-hold periods but edge-replicas were not taken in this particular experiment. Acoustic emission activity was detected

during this period and the rate of acoustic emission emanating from the test specimen was found to be a function of the magnitude of the applied load.

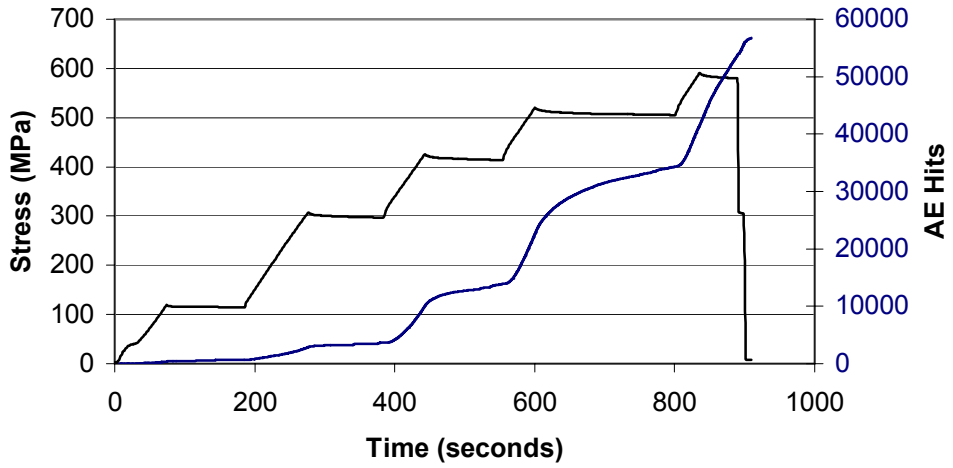

Figure 7 AE hits generated during ramp and hold periods.

A number of FOS were evaluated, including sensors that were bonded to the composite using different bonding techniques. Figure 8 and Figure 9 present the data from an epoxy bonded and silicone bonded FOS respectively.

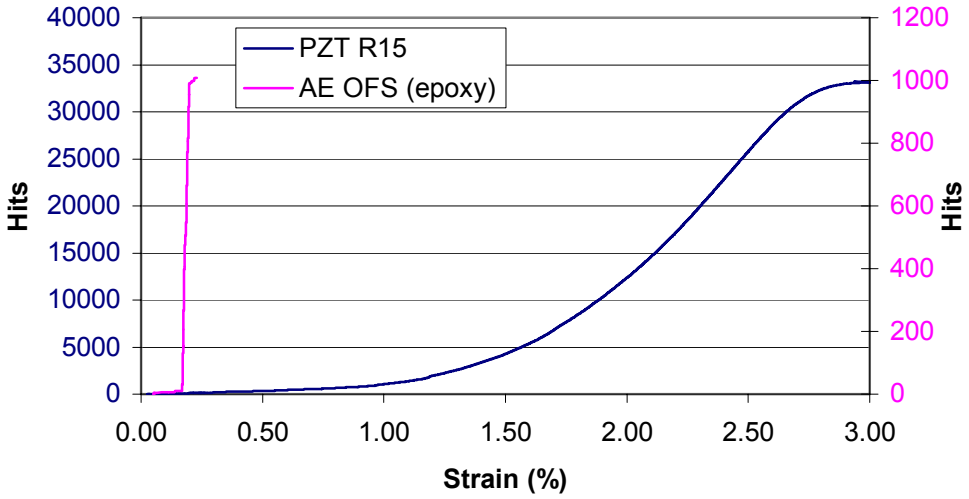

Figure 8 Comparison of PZT (R15) with epoxy bonded AE OFS.

Figure 8 presents the 'hits' detected by an optical sensor that had been bonded to the composite using epoxy adhesive. It is important to note that the optical sensor failed mechanically at ~ 0.25 % strain, and upon examination evidence of cracking of the sensor housing due to stress was seen. This behaviour is typical for the other epoxy bonded sensors with failure strains of between 0.2 – 0.5 %. The use of a rigid epoxy bond succeeded in transferring stress from the composite to the sensor but has the side effect that sensors bonded in this manner may only be placed in relatively low static strain regions.

Figure 9 presents typical AE data for an optical sensor surface mounted using silicone and compared with representative data from an R15 PZT transducer. For this data the R15 transducer had an amplitude threshold of 63 dB applied, as this was the approximate minimum sensitivity of the optical sensor. It can be seen from Figure 6 that the threshold applied will alter the shape of the hits against strain curve due to the characteristic emission amplitude varying with the different

damage modes in the composite – the selection of this threshold allows a more direct comparison to be made.

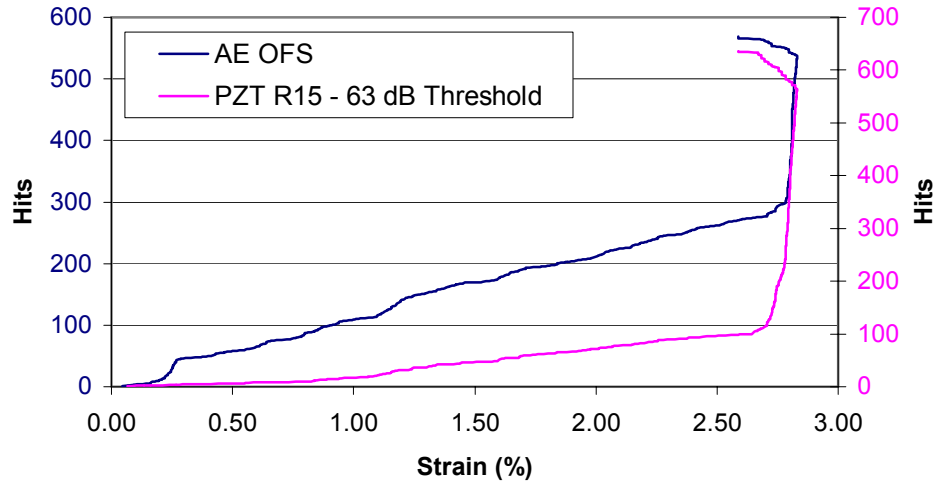

Figure 9 Comparison of AE data from PZT (R15), threshold set at 63 dB, and silicone bonded AE OFS.

On examination of Figure 9 it can be c seen that the optical sensor has a similar response to AE as the PZT transducer. It is important to note that the sensors bonded with silicone survived until the composite failure strain (~3 %) and is probably due to the less efficient strain transfer to the sensor housing. This is an important factor in the selection of the bonding material as the interface must fulfil two criteria; to enable efficient stress transfer to the sensor for increased sensitivity and to reduce the static strain level experienced by the sensor to within its limits. This interface is critical to the operation and repeatability of the sensor and is currently being investigated.

Edge replicas were taken from selected specimens at strain levels of 0, 0.4, 1.25, 1.8, 2.2 and 2.6 % and respresentative images are shown in Figure 10. From the replica at 0 % strain it can be observed that there is no evidence of the composite having any existing cracking or delamination.

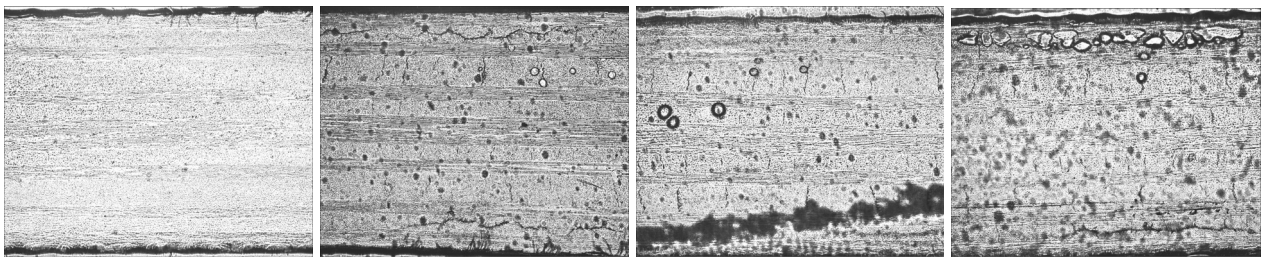

Figure 10 Edge replicas of composite coupon taken at strain intervals of 0, 1.25, 1.8 and 2.6 % strain respectively.

From the edge replica taken at 0.4 % (not shown) strain delamination was observed in the 0°/90° (1/2) ply but no transverse cracks were observed in the edge replication region. The edge replication taken at 1.25 % showed initiation of transverse cracks in the 90°/90° (4/5 and 12/13) plies and propagation of a delamination crack in the 0°/90° interface (1/2 plies). Correspondingly (Figure 6), an increase in acoustic amplitude was observed. At 1.8 % strain transverse crack initiation in 90° plies (7th and 10th ply) and more transverse crack initiation and crack propagation through the 90°/90° plies were observed. It was also observed that the transverse cracks in the 90°/90° plies (4/5 and 12/13) start initiating interlaminar (delamination) cracks between the adjoining 0° plies (3,6 and 11,14). The delamination crack in 0°/90° interface (1/2 and 15/16) propagates through the length of the composite. From the edge replication taken at 2.2 % propagation of transverse cracks and delamination in 90°/90° plies and 0°/90° plies respectively were observed. The spacing between the

transverse cracks in 90°/90° plies were found to decrease as the load increases; additionally increases in crack length were also observed. At 2.6 % strain delamination in the 0°/90° plies were observed and the crack spacing in the transverse plies appears to have reached saturation; correspondingly, there was a reduction in the acoustic energy release and the amplitude monitored. Soon after this stage the specimen failed. This catastrophic damage of composite resulting from the combination of transverse cracking, delamination, fibre splitting and breakage can be observed from the high acoustic energy and amplitude from the PZT sensors at this high stress (Figure 6).

This observed failure sequence correlates closely with the measured optical signal in Figure 9. This data shows the expected increase in high amplitude 'hits' approaching composite failure.

4. CONCLUSIONS

The use of a FOS for AE detection has been demonstrated. Correlation between the AE detected using a conventional PZT transducer and the FOS has been obtained.

The AE events generated during quasi-static testing of a composite coupon and measured using both an optical and PZT transducer, can be related to the damage events observed from edge replication.

The FOS showed a lower sensitivity to AE than the PZT, and it was shown that this sensitivity is critically controlled by the sensor to substrate bonding conditions. Future work will concentrate on optimising this interface for specific applications.

ACKNOWLEDGEMENTS

The authors would like to acknowledge the support given to this work by the EPSRC, DTI LINK (FOASMIE), UK MOD and the Centre for Photo-Analysis and Photo-Manipulation of Materials at Cranfield University.

References:

1. **Butler T., Chen R., Krishnamurthy S., Badcock R.A.** and **Fernando G.F.**, "A low-cost fiber optic acoustic emission sensor for damage detection in engineering composite materials and structures", *Proceedings of the Fourth International Workshop on Structural Health Monitoring*, Stanford University, **September 15-17**, 2003, 1117-1124.